

Bone regeneration capacities of alveolar bone mesenchymal stem cells sheet in rabbit calvarial bone defect

Journal of Tissue Engineering
Volume 11: 1–12
© The Author(s) 2020
Article reuse guidelines:
sagepub.com/journals-permissions
DOI: 10.1177/2041731420930379
journals.sagepub.com/home/tej



Yanan Liu^{*1,2,3} , Haifeng Wang^{*2}, Huixin Dou¹, Bin Tian³ ,
Le Li⁴, Luyuan Jin¹, Zhenting Zhang³ and Lei Hu^{1,3}

Abstract

Mesenchymal stem cells sheets have been verified as a promising non-scaffold strategy for bone regeneration. Alveolar bone marrow mesenchymal stem cells, derived from neural crest, have the character of easily obtained and strong multi-differential potential. However, the bone regenerative features of alveolar bone marrow mesenchymal stem cells sheets in the craniofacial region remain unclear. The purpose of the present study was to compare the osteogenic differentiation and bone defect repairment characteristics of bone marrow mesenchymal stem cells sheets derived from alveolar bone (alveolar bone marrow mesenchymal stem cells) and iliac bone (Lon-bone marrow mesenchymal stem cells) *in vitro* and *in vivo*. Histology character, osteogenic differentiation, and osteogenic gene expression of human alveolar bone marrow mesenchymal stem cells and Lon-bone marrow mesenchymal stem cells were compared *in vitro*. The cell sheets were implanted in rabbit calvarial defects to evaluate tissue regeneration characteristics. Integrated bioinformatics analysis was used to reveal the specific gene and pathways expression profile of alveolar bone marrow mesenchymal stem cells. Our results showed that alveolar bone marrow mesenchymal stem cells had higher osteogenic differentiation than Lon-bone marrow mesenchymal stem cells. Although no obvious differences were found in the histological structure, fibronectin and integrin $\beta 1$ expression between them, alveolar-bone marrow mesenchymal stem cells sheet exhibited higher mineral deposition and expression levels of osteogenic marker genes. After being transplanted in the rabbit calvarial defects area, the results showed that greater bone volume and trabecular thickness regeneration were found in bone marrow mesenchymal stem cells sheet group compared to Lon-bone marrow mesenchymal stem cells group at both 4 weeks and 8 weeks. Finally, datasets of bone marrow mesenchymal stem cells versus Lon-bone marrow mesenchymal stem cells, and periodontal ligament mesenchymal stem cells (another neural crest derived mesenchymal stem cells) versus umbilical cord mesenchymal stem cells were analyzed. Total 71 differential genes were identified by overlap between the 2 datasets. Homeobox genes, such as *LHX8*, *MKX*, *PAX9*, *MSX*, and *HOX*, were identified as the most significantly changed and would be potential specific genes in neural crest mesenchymal stem cells. In conclusion, the Al-bone marrow mesenchymal stem cells sheet-based tissue regeneration appears to be a promising strategy for craniofacial defect repair in future clinical applications.

Keywords

Alveolar bone marrow stem cells, bone regeneration, calvarial defect, mesenchymal stem cells

Date received: 20 February 2020; accepted: 9 May 2020

¹Beijing Key Laboratory of Tooth Regeneration and Function Reconstruction, School of Stomatology, Capital Medical University, Beijing, China

²Department of Stomatology, Beijing Bo'ai Hospital, China Rehabilitation Research Center, School of Rehabilitation, Capital Medical University, Beijing, China

³Department of Prosthodontics, School of Stomatology, Capital Medical University, Beijing, China

⁴Department of Stomatology, Tsinghua University Hospital, Beijing, China

*These authors contributed equally to this work.

Corresponding authors:

Lei Hu, Beijing Key Laboratory of Tooth Regeneration and Function Reconstruction, School of Stomatology, Capital Medical University, Tian Tan Xi Li No.4, Beijing 100050, China.
Email: hulei@cmmu.edu.cn

Zhenting Zhang, Department of Prosthodontics, School of Stomatology, Capital Medical University, Tian Tan Xi Li No.4, Beijing 100050, China.
Email: 13601324515@163.com



Introduction

Craniofacial bone defect is a common disease, which would seriously affect the health of patients and brings difficulties for medical treatment. Currently, autogenous bone, autografts and allografts substitutes are the standard treatments for bone tissue reconstruction, but with many drawbacks. The autogenous bone practical clinical application is restricted by both donor site morbidity and the limited availability of bone volume.¹ Besides, commercial bone grafts substitutes have poor efficiency in large bone defect reconstruction with the limited osteogenic and osteoinductive ability.² In recent decades, stem cell-based tissue engineering has emerged as a therapeutic approach to repair of bone defects.³ The stem cell-based tissue engineering depends on biomaterials and stem cells. Although substantial advances have been made, there are many challenges in craniofacial bone tissue engineering, such as complex physiological structures, suitable biomaterials and superior osteoinductive stem cells.⁴

Recently, cell sheet engineering has been developed as a unique, scaffold-free method of tissue regeneration,⁵ with the advantage of maintenance of extracellular matrix (ECM) and cell-cell junctions, without the impairment induce by biomaterial and its degradation.⁶ Since the mesenchymal stem cells (MSCs) sheets were first used for the regeneration of osteogenic tissue in 2006,⁷ more and more studies have been made to investigate the function of MSC sheet in craniofacial bone regeneration. By being used alone or in conjunction with exogenous biomaterials, MSCs sheets have been verified effective in bone regeneration.⁸ Bone marrow MSCs (BMSCs), with the character of high proliferation and osteogenic capacity, are the predominant MSCs used in preclinical and clinical studies of cell sheet based craniofacial tissue regeneration.⁹ However, several disadvantages of BMSCs have been found in the application, such as the invasive and painful harvest procedure, impairment of self-renewal and differentiation capacity due to donor age,¹⁰ and weak stemness maintenance during expansion *in vitro*, as well as inflammation stimulation.¹¹

Generally, the BMSCs are majorly derived from iliac crest bone marrow. They were also discovered in alveolar bone, which are named alveolar bone MSCs (Al-BMSCs), have the potential of osteogenic, chondrogenic or adipogenic differentiation,¹² and can effectively regenerate bone tissue *in vivo*.¹³ Compared with other MSCs, Al-BMSCs have the advantage of less invasive and easier harvest procedures, high proliferation capacity, and stronger bone formation than iliac BMSCs,¹⁴ thus have emerged as a potential cell source for bone tissue engineering.¹⁵ It has also been found that Al-BMSCs can be induced to cell sheets, and can increase local bone density when transplanted into the tooth-extraction site.¹⁶ However, although several studies have compared the character of Al-BMSCs

and BMSCs *in vitro* and *in vivo*, most studies are in animal models, only a few articles are relevant to human study. In addition, the difference of Al-BMSCs sheet and BMSCs sheet *in vitro* and the craniofacial bone defect repairment features *in vivo* remain unclear.

The purpose of this study was to compare the histology character, osteogenic differentiation, and specific gene expression of BMSCs sheets derived from alveolar bone (Al-BMSCs) and iliac bone (Lon-BMSCs) *in vitro*. Then to investigate the bone defect repairment characteristics *in vivo* with Al-BMSCs sheet and Lon-BMSCs sheet in a rabbit calvarial defect model.

Materials and methods

Rabbit

10 adult female New Zealand white rabbits weighing between 3.0 and 3.5 kg were used in this study. The animal study was approved by the Animal Care and Use Committee of Beijing Stomatological Hospital, Capital Medical University (Ethical code: KQYY-201812-002). The rabbits were purchased from Beijing Fang Yuanyuan Laboratory Animal (Beijing, China) and maintained in a specific pathogen-free animal facility and kept under conventional conditions with free access to water and food.

BMSCs derived from iliac bone and alveolar bone cultures

BMSCs derived from alveolar bone (Al-BMSCs) were cultured from bone marrow complex during the preparation of the implant hole according to the previous study.¹⁷ Briefly, the bone marrow complex (about 0.1–0.2 mL) were obtained from dental implant treatment of five healthy male patients (30–50 years old), with their consent and approval from the Ethics Committee of China Rehabilitation Research Center (No. 2018-094-1). The bone marrow complex was put into the centrifugal tubes with medium and were grown in alpha-MEM (Invitrogen, Carlsbad, CA, USA), supplemented with 15% fetal bovine serum (FBS; Invitrogen, Carlsbad, CA, USA), 2 mmol/L glutamine, 100 U/mL penicillin, and 100 µg/mL streptomycin (Invitrogen, Carlsbad, CA, USA) in a humidified incubator under 5% CO₂ at 37°C. The culture medium was changed every 3 days.

The human BMSCs extracted from iliac bone marrow (Lon-BMSCs) were obtained from the Department of Experimental Hematology, Beijing Institute of Radiation Medicine. The Lon-BMSCs and Al-BMSCs were expanded by detachment with 0.5% trypsin- ethylenediaminetetraacetic acid (EDTA) solution when the respective cultures reached 80% confluence. All the cells at passages 3–5 were used in subsequent experiments.

Stem cell sheet induction and histological observation

To induce the cell sheets, Lon-BMSCs and AI-BMSCs at third passages were sub-cultured in 10 cm dishes with 2×10^5 cells/well, and cultured in complete medium containing 20 $\mu\text{g}/\text{mL}$ vitamin C.¹⁸ About 10 days later, the cells on the edge of the dishes wrapped, indicating that cell sheets had formed. After detaching the cell sheets were fixed with 4% formalin and then embedded in paraffin. Sections (8- μm) were prepared, deparaffinized, and stained with hematoxylin-eosin (HE).

Osteogenesis potential detection

To evaluate the osteogenic differentiation potential, Lon-BMSCs and AI-BMSCs or Lon-BMSCs and AI-BMSCs sheets were incubated in the osteogenic medium (Invitrogen). The medium was changed every 2 days. On day 5 after induction, cells or cell sheets were fixed with 4% paraformaldehyde for alkaline phosphatase (ALP) staining following the manufacturer's protocol (Sigma-Aldrich). On day 14 after induced for osteogenic induction, cells or cell sheets were fixed with 70% ethanol, and stained with solution contained 2% Alizarin Red (Sigma-Aldrich). ALP and Alizarin Red staining were measured by using the Image-Pro Plus 6.0 program (Media Cybernetics, Rockville, MD, USA).

Real-time PCR for assessing gene expression

Cells or cell sheets were treated with Trizol (Invitrogen). Total mRNA was extracted by RNAprep pure Cell Kit (TIANGEN, Beijing, China). Then cDNA was synthesized with FastQuant RT Kit (TIANGEN, Beijing, China). We obtained GAPDH primer, forward 5'-CGGACCAATACGACCAAATCCG -3,' reverse 5'-AGCCACATCGCTCAGACACC -3'; OPN primer, forward 5'- ATGATGGCCGAGGTGATAGT-3,' reverse 5'- ACCATTCAACTCCTCGCTTT-3'; OCN primer, forward 5'- AGCAAAGGTGCAGCCTTTGT-3,' reverse 5'-GCGCCTGGGTCTCTTCACT-3'; Runx2 primer, forward 5'- TCTTAGAACAAATTCTGCCCTTT-3,' reverse 5'-TGCTTTGGTCTTGAAATCACA-3'; BSP primer, forward 5'- CAGGCCACGATATTATCTTTACA-3,' reverse 5'- CTCCTCTTCTTCTCCTCCTC-3,' from Primer 3. Real-time polymerase chain reaction (PCR) reactions were performed with the SuperReal PreMix Plus SYBR Green PCR kit (TIANGEN, Beijing, China).

Cell sheets transplantation in Rabbit Calvarial Bone Defect model

Ten rabbits were anesthetized via intramuscular injection with 7.5 mg/kg tiletamine-zolazepam (Zoletil 50, Virbac,

Carros Cedex, France) and 2 mg/kg xylazine hydrochloride (Sumianxin II, Jilin Huamu, Changchun, China). The rabbit calvarial bone defect was created according to the previous study.¹⁹ After midline skin incision, muscle dissection, and periosteal elevation, the calvarial bone was carefully exposed. Two symmetrical round defects, each 5 mm in diameter and 2 mm in depth, were prepared in the calvaria using a trephine bur under the copious irrigation of sterile saline. Two experimental modalities were randomly allocated to the 20 defects, as follows: (1) Lon-BMSCs sheet and (2) AI-BMSCs sheet. Cell sheets were collected and immediately implanted into the bone defects. After incision closed, the animals received 30 mg/kg penicillin by intramuscular injection to prevent infection. The animals had free access to food and water and were monitored daily for any complications or abnormal behaviors during the healing period.

Sequential fluorescent labeling

According to the time of execution, the experimental animals were divided into two groups ($n=5$). In the 4-week group, the animals were intramuscularly injected with 90 mg/kg Xylenol orange (Sigma, USA), 20 mg/kg calcein (Sigma, USA), and 30 mg/kg alizarin red S (Sigma, USA), respectively, at 1, 2, and 3 weeks after the operation. In the 8-week group, the time point was 2, 4, and 6 weeks.

Micro-computed tomography measurements

After 4 and 8 weeks of healing, the rabbits were sacrificed. The skull bones were harvested and fixed in 10% neutral buffered formalin, the samples were processed and scanned with a micro-CT (Siemens Inveon, Siemens, Germany) running at a voltage of 80 kV, an electric current of 500 mA, exposure time of 2000 ms and a pixel resolution of 15 μm with a 0.5 mm aluminum filter. Three-dimensional (3D) image models were reconstructed using Inveon Research Workplace 4.2 (Siemens, Germany). A 5 mm diameter circular region was placed in the center of the initial defect area and was defined as the region of interest (ROI). The optimal threshold for discriminating between the bone and grafting materials was determined as 615. Finally, the bone volume density (BV/TV %) within the ROI, was determined and expressed as mean \pm standard deviation ($M \pm SD$).

Histology analysis

For hard tissue slices examination, samples were dehydrated with ethanol of ascending concentrations, embedded in polymethylmethacrylate (PMMA) and cut into sections using a microtome (LEICA SP1600, Germany). The fluorescent labeling was observed using the Stereo Microscope and Laser Scanning Confocal Microscope

(OLYMPUSFV1000, Japan). The area of three fluorescent stained bone was quantified by Image-Pro Plus 6.0 software. For HE staining, the samples were decalcified in 10% EDTA (pH 7.0) for 21 days, stained with HE (Sigma, St. Louis, MO) following standard protocols, and observed using a standard light microscope Leica DM 4000 microscope (Leica, Germany).

Immunofluorescence analysis

For fluorescent immunohistochemistry (IHC) of fibronectin and integrin $\beta 1$, deparaffinized slides were subjected to antigen retrieval in boiled sodium citrate buffer solution (pH 6.0) for 10 min, then blocked for 20 min in blocking buffer (5% bovine serum albumin and 0.01% Triton X-100 in phosphate buffer solution (PBS; Sigma). After blocking, samples were incubated with rabbit polyclonal anti-fibronectin (Abcam, ab2413, 1:300) and rabbit polyclonal anti-integrin $\beta 1$ (Abcam, ab183666, 1:300) overnight at 4°C. Alexa Fluor 594 goat anti-rabbit IgG (Life Technologies, USA, 1:500) were used to detect primary antibodies, and then counterstained with 4',6-diamidino-2-phenylindole (DAPI; Invitrogen). Immunofluorescent images were captured using a Leica TCS SP5 confocal microscope (Leica). The expression intensity was measured using the Image-Pro Plus 6.0 program (Media Cybernetics, Rockville, MD, USA).

Bioinformatics analysis gene expression profile of Lon-BMSCs and AI-BMSCs

Gene expression dataset GSE58474 was downloaded from the Gene Expression Omnibus (GEO) database, which compared the gene expression between human AI-BMSCs and Lon-BMSCs. More gene expression data were derived from S Yu et al.,²⁰ which compared the gene expression between human periodontal ligament mesenchymal stem cells (PDLSCs) and umbilical cord MSCs (UCMSCs). Those genes with an adjusted P-value < 0.05 and the absolute value of fold-change (FC) > 2 were analyzed. Then differentially expressed genes were subjected to Gene Ontology (GO) and The Kyoto Encyclopedia of Genes and Genomes (KEGG) analysis to explore the gene function of individual genomic products based on defined features and understand the biological meaning underlying particular gene lists. In this study, both GO and KEGG analyses of differentially expressed genes were performed with a criterion false discovery rate (FDR) < 0.05 .

Statistical analysis

All statistical calculations were performed. All values are described as the mean \pm standard deviation (M \pm SD). Statistics were calculated by using SPSS 13.0 statistical software. Student t-test was used to determine statistical significance. $P \leq 0.05$ was considered statistically significant.

Results

Higher osteogenic differentiation of AI-BMSCs compared to Lon-BMSCs

AI-BMSCs and Lon-BMSCs were derived from 5 individuals, the stem cells were identified by flow cytometric analysis and osteogenesis differentiation (Supplemental Figure 1). Both the ALP staining and Alizarin Red staining showed AI-BMSCs have higher osteogenic differentiation compared to Lon-BMSCs (Figure 1(a), (b)). The results of RT-PCR showed that the expression of BSP, OPN, OCN, Runx2 were higher expressed in AI-BMSCs than Lon-BMSCs at 0 day, 7 days and 14 days of osteogenic induction (Figure 1(c-f)), at 28 days, the expression of OPN and OCN were also up-regulated in AI-BMSCs than Lon-BMSCs (Supplemental Figure 2).

Histological analyses of Lon-BMSCs and AI-BMSCs sheets

Cell sheets were formed after 10 days of culture (Figure 2(a), (b)). Histological analysis showed that both sheets consisted of 2–3 layers of cells, which were closely connected (Figure 2(c, d)). The immunofluorescence staining indicated that there was no significant difference in the expression of fibronectin and integrin $\beta 1$ between Lon-BMSCs and AI-BMSCs sheets (Figure 2(e-h), Supplemental Figure 3A).

Higher osteogenic differentiation of AI-BMSCs sheet than Lon-BMSCs sheet

AI-BMSCs and Lon-BMSCs derived from 5 individuals were induced to cell sheet. The result of ALP staining and Alizarin Red staining showed AI-BMSCs sheets have higher osteogenic differentiation compared to Lon-BMSCs sheet (Figure 3(a, b), Supplemental Figure 3B, C). The results of RT-PCR showed that the expression of BSP, OPN, OCN, Runx2 were higher expressed in AI-BMSCs sheet than Lon-BMSCs sheet at 0 day and 7 days osteogenic induction (Figure 3(c-f)). The results showed AI-BMSCs sheets have higher osteogenic differentiation than Lon-BMSCs sheets, although the difference was decreased at 14 days of osteogenic induction.

Bone regeneration characteristics of Lon-BMSCs and AI-BMSCs sheets in rabbit calvarial defects

In the calvarial defect rabbit model, it cannot be repaired by self-healing (Supplemental Figure 3D, E). The skull bones were harvested at 4 and 8 weeks. Regeneration of the calvarial defects was evaluated using micro-CT. The 3D reconstruction of the images showed that the bone defect area was decreased when transplanted with Lon-BMSCs and

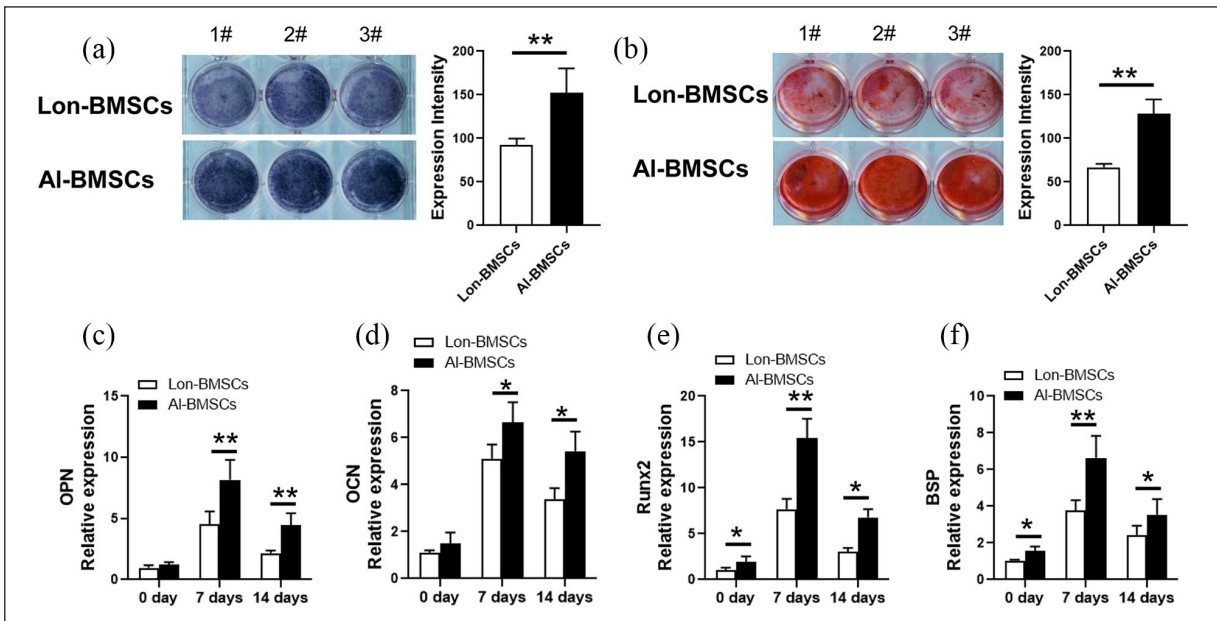


Figure 1. Comparison of osteogenic differentiation capacities of Lon-BMSCs and AI-BMSCs. (a) ALP (alkaline phosphatase) staining and qualitative measurement of Lon-BMSCs and AI-BMSCs following 7 days of osteogenic induction. (b) Alizarin red staining and qualitative measurement of Lon-BMSCs and AI-BMSCs following 14 days of osteogenic induction. (c, d, e, and f) Real-time PCR showed the expression of OPN, OCN, Runx2 and BSP were up-regulated in AI-BMSCs compared to Lon-BMSCs. GAPDH was used as an internal control. Student's t-test was used to determine statistical significance. Values are mean \pm SD, Error bars represent the s.d. (n = 5), *P \leq 0.05, **P \leq 0.01.

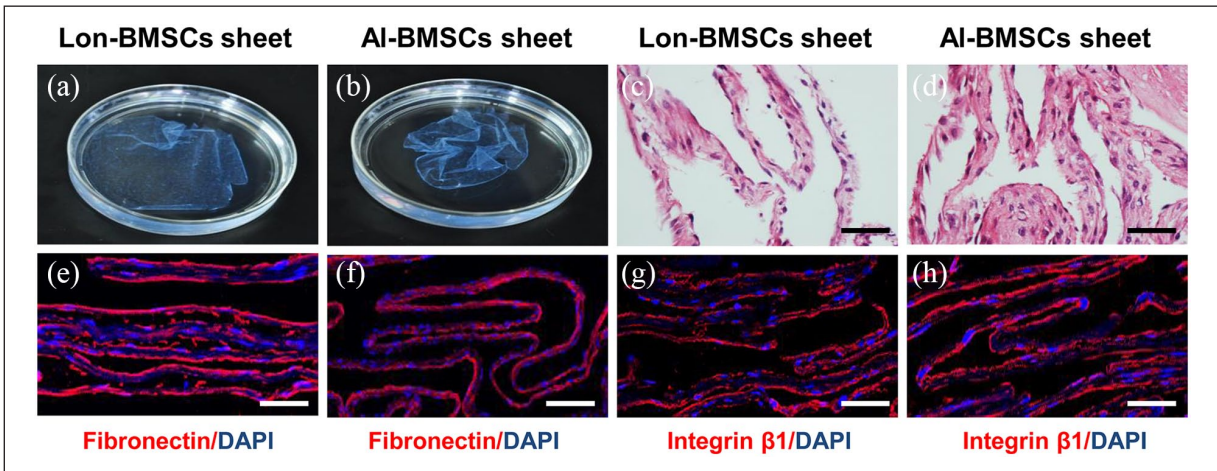


Figure 2. Histological analyses of Lon-BMSCs and AI-BMSCs sheets. (a, b) The gross morphology of Lon-BMSCs and AI-BMSCs sheet showed no difference, with Vit C induced for 10 days. (c, d) The Hematoxylin and eosin (HE) staining of Lon-BMSCs and AI-BMSCs sheet all sheets consisted of 2-3 layers of cells. (n = 5; scale bar: 100 μ m). Immunofluorescence analysis showed (e, f) fibronectin and (g, h) integrin β 1 were highly expressed in the Lon-BMSCs and AI-BMSCs sheets, with no significant difference between them. Sections were counterstained with DAPI (blue). (n = 5, scale bar: 100 μ m).

AI-BMSCs sheet at 4 weeks. More newly formed bones were witnessed in AI-BMSCs sheet transplanted group than Lon-BMSCs sheet group (Figure 4(a)). The BV/TV (bone volume/tissue volume) ratios (Figure 4(b)), and trabecula thickness (Figure 4(d)) in the defect areas of the AI-BMSCs sheet group were significantly higher than Lon-BMSCs sheet group (P < 0.05), while the BSA/BV (bone surface/

bone volume) ratios (Figure 4(c)) in the defect areas of the AI-BMSCs sheet group were significantly lower than Lon-BMSCs sheet group (P < 0.05). HE staining and sequential fluorescent labeling showed much more new bone formation was formed and diminishes the diameter of the defect in AI-BMSCs sheet group than Lon-BMSCs sheet group (Figure 4(e, f)). Larger regenerated tissues were found in

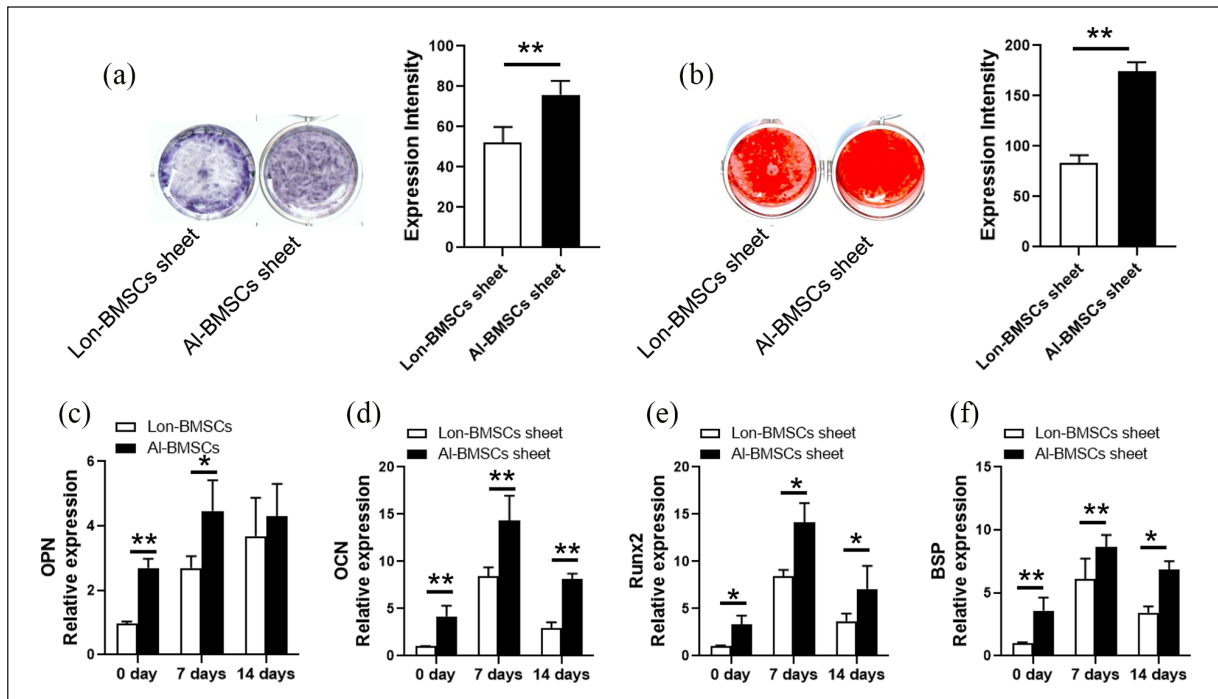


Figure 3. Comparison of osteogenic differentiation capacities of Lon-BMSCs sheet and AI-BMSCs sheet. (a) ALP staining and qualitative measurement showed AI-BMSCs and Lon-BMSCs sheets following 7 days of osteogenic induction. (b) Alizarin red staining and qualitative measurement of AI-BMSCs and Lon-BMSCs sheets following 14 days of osteogenic induction. (c, d, e) Real-time PCR showed the expression of OPN, OCN, Runx2 and BSP were up-regulated in AI-BMSCs sheet compared to Lon-BMSCs sheet. GAPDH was used as an internal control. Student's t-test was used to determine statistical significance. Values are mean \pm SD, Error bars represent the s.d. (n=5), *P \leq 0.05, **P \leq 0.01.

AI-BMSCs sheet group than Lon-BMSCs sheet group (P < 0.05) (Figure 4(g)). T-bet (Th1 marker), CCR7 (type I macrophage marker) and CD206 (type II macrophage marker) were analyzed by IHC analysis. At 4 weeks the count of Th1, M1 and M2 were witnessed in blank control, Lon-BMSCs sheet and AI-BMSCs sheet group, without any difference (Supplemental Figure 4).

At 8 weeks, much great bone formation was found both in AI-BMSCs and Lon-BMSCs sheet groups, but the data showed the similar tendency of 4 weeks, more newly formed bones were witnessed in AI-BMSCs sheet group compared to Lon-BMSCs sheet group (Figure 5).

Identification of key genes and pathways specific in AI-BMSCs using an integrated bioinformatics analysis

AI-BMSCs and dental MSCs (PDLSCs, dental pulp stem cells (DPSCs), SCAPs, etc.) are derived from the neural crest, and they have similar characteristics. Though integrated bioinformatics analysis with other neural crest derived MSCs, it would reveal the key genes and pathways in neural crest derived MSCs compared to other tissue derived MSCs. The published gene expression datasets between human AI-BMSCs and Lon-BMSCs, and the gene expression between human PDLSCs and Umbilical Cord MSC (UCMSCs) were used. The results showed a

total 173 significantly changed genes were identified (94 up-regulated and 79 down-regulated) in AI-BMSCs compared to Lon-BMSCs (Figure 6(a)). While total 1059 significantly changed genes were identified (588 up-regulated and 471 down-regulated) in PDLSCs compared to UCMSCs (Figure 6(b)). Total 71 genes overlapped across the two datasets, suggesting that these genes may be conserved in neural crest derived MSCs. Among these 71 genes, 41 were up-regulated while 29 were down-regulated (Table). GO and KEGG analyses were performed on the 71 genes. The GO analysis revealed that most of the proteins encoded by these differentially expressed genes were ECM proteins located in the extracellular space (Figure 6(c)). The molecular functions (MF) enriched in this dataset were primarily associated with platelet-derived growth-factor binding and ECM structural constitution, while the enriched biological processes (BP) were primarily those associated with ECM organization and cell adhesion. The KEGG analysis revealed that the primary enriched signaling pathways were associated with ECM-receptor interaction, protein digestion and absorption, focal adhesion, and the PI3K-Akt signaling pathway (Figure 6(d)). Interestingly, the Homeobox genes like *LHX8*, *MKX*, *PAX9*, *MSX* and *HOX*, were identified as the most significantly changed, suggesting that their distinctive function in neural crest derived MSCs and tissue development.

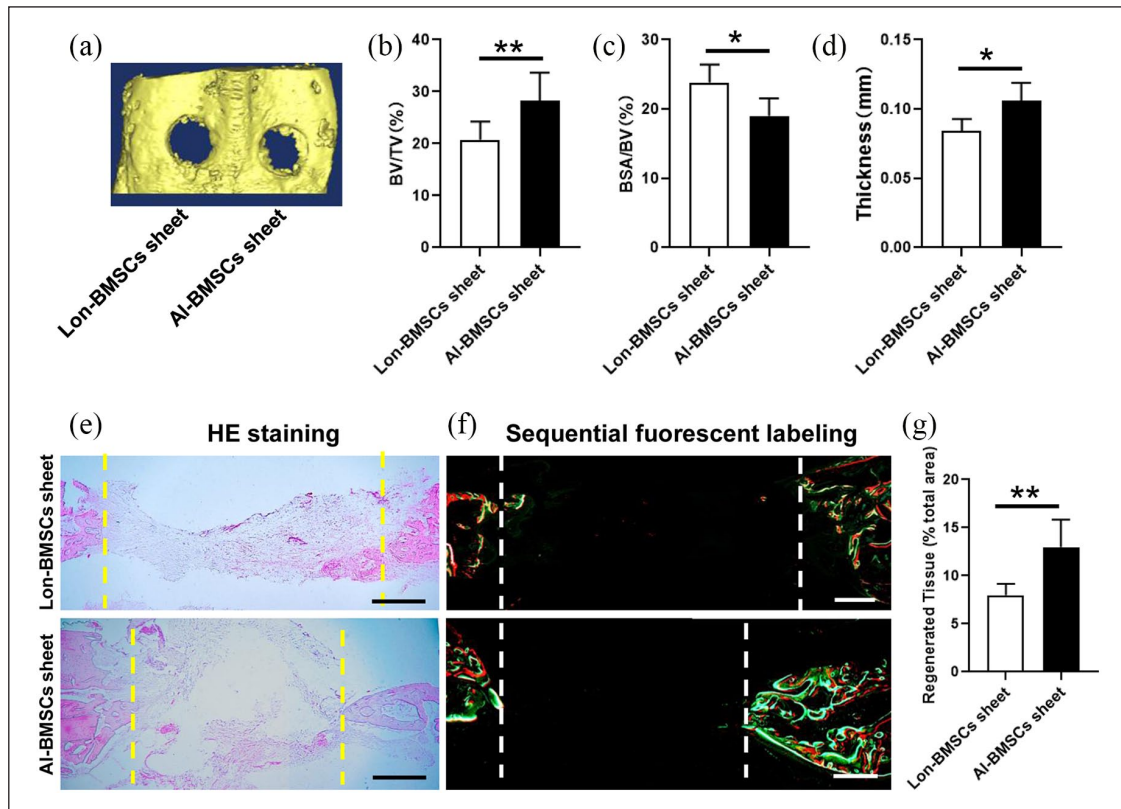


Figure 4. Analyses of bone defect repair by Lon-BMSCs and AI-BMSCs sheets in rabbit calvarial defect at 4 weeks. (a) 3D-reconstruction of Micro-CT images of defect regions in Lon-BMSCs and AI-BMSCs sheet at 8 weeks. (b, c, d) Qualitative measurement of BV/TV, BSA/BV and thickness values between Lon-BMSCs and AI-BMSCs sheets groups (* $P < 0.05$, ** $P < 0.01$). (e) HE stained images of bone defect regions at 8 weeks in Lon-BMSCs and AI-BMSCs sheets groups. (f) Sequential fluorescent labeling of bone formation and mineralization. Bone formation and mineralization in the defect area of the rabbit at 8 weeks. Red, green and yellow represent labeling by Alizarin Red S, Calcein and Xylenol orange. (g) New bone area percentages in the defect region were assessed by histomorphometric analyses. (Scale bars = 0.5 mm) (* $P < 0.05$, ** $P < 0.01$).

Discussion

In the present study, our results showed AI-BMSCs have higher osteogenic differentiation than Lon-BMSCs. AI-BMSCs can be induced to cell sheet with Vit C, with the similar histological structure and containing ECM protein (fibronectin and integrin $\beta 1$) to Lon-BMSC. But AI-BMSCs sheet showed higher osteogenic differentiation capacity and bone defect reconstruction in rabbit calvarial defect model. Like other neural crest derived MSCs, Homeobox genes, such as *LHX8*, *MKX*, *PAX9*, *MSX* and *HOX*, were specifically highly expressed in AI-BMSCs. All the results showed AI-BMSCs sheet based tissue regeneration would a promising strategy for craniofacial defect repair in future clinical applications and Homeobox genes have distinctive functions in neural crest derived MSCs and tissue development.

Canonical stem cell based bone engineering is dependent on stem cells and materials. After further research, many drawbacks have been found. This strategy needs culturing and expanding cells, which would destroy the ECM and intercellular connections between cells. ECM contains

many necessary bioactive molecules for cells and tissues homeostasis,^{21,22} and the destruction of ECM can impair tissue regeneration efficiency *in vivo*. Besides, the transplanted scaffolds may induce local tissue inflammation, and cell necrosis by impairing nutrients and oxygen diffusion, as well as the occurrence of inflammation.^{6,23} Therefore, scaffold-free tissue regeneration strategy was emerged to avoid these limitations.^{6,23} Cell sheet technology is a promising alternative engineering technique, in which the 2–3 layers structure was formed when cells were hyper confluent.²⁴ This strategy preserves cell-cell interactions and the ECM from the destruction by enzymatic digestion. The ECM, which contains many ingredients, such as cell–cell junctions, adhesion molecules, growth factor receptors and ion channels, not only offers the supplements for cell survival maintains, but also mediates direct adhesion of the sheet to the target organ,²⁵ which would benefit the cell anchoring. Besides, cell sheet technology can avoid the inflammatory reaction caused by the degradation of scaffold, which would produce acidic substances which will hinder cell migration and lead to the

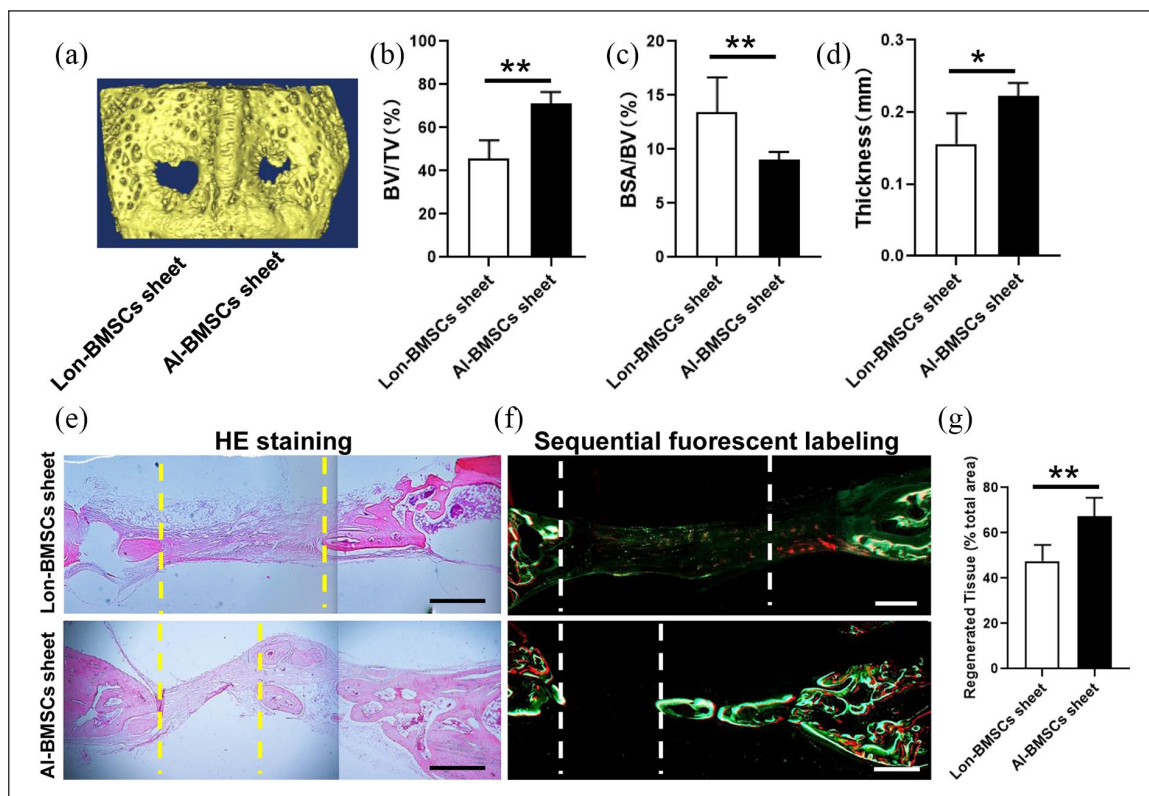


Figure 5. Analyses of bone defect repairment by Lon-BMSCs and AI-BMSCs sheets in rabbit calvarial defect at 8 weeks. (a) 3D-reconstruction of Micro-CT images of defect regions in Lon-BMSCs and AI-BMSCs sheet at 8 weeks. (b, c, d) Qualitative measurement of BV/TV, BSA/BV and thickness values between Lon-BMSCs and AI-BMSCs sheets groups (* $P < 0.05$, ** $P < 0.01$). (e) HE stained images of bone defect regions at 8 weeks in Lon-BMSCs and AI-BMSCs sheets groups. (f) Sequential fluorescent labeling of bone formation and mineralization. Bone formation and mineralization in the defect area of the rabbit at 8 weeks. Red, green and yellow represent labeling by Alizarin Red S, Calcein and Xylenol orange. (g) New bone area percentages in the defect region were assessed by histomorphometric analyses. (Scale bars = 0.5 mm) (* $P < 0.05$, ** $P < 0.01$).

reduction of cell activity.²⁶ The cell sheet has certain mechanical strength and operability, and the ideal thickness of the sheet can be constructed by means of superposition, it can be implanted into the biological body by means of tamping and injection, regardless of the size of the scaffold.²⁷ Thus, cell sheet could recreate a similar natural biological microenvironment for tissue regeneration.

To date, cell sheets have been widely used in tissue engineering, including craniofacial bone⁸ and dental tissue.^{18,28} Like PDLSCs and DPSCs have been successfully used for periodontal regeneration.^{29,30} Our previous studies have shown that PDLSC sheet can also be used for bio-root regeneration.^{31,32} MSC sheets first used for the regeneration of osteogenic tissue were described in 2006.⁷ Subsequently, many research groups have reported bone formation or regeneration by the BMSCs sheet itself.³³ In order to enhance the bone regenerated capacity of MSCs sheet, many methods have been used to combine with MSCs sheet,³⁴ like HA/TCP, chitosan/hyaluronic acid nanoparticles plus microRNA-21, nanoscale HA combined with autologous platelet-rich fibrin, as well as various biological agents.⁹

Lon-BMSCs were the major MSCs used in previously MSCs sheet based bone reconstruction.³⁵ Recently, numerous types of neural crest derived-MSCs have been isolated and characterized, including PDLSCs, DPSCs, stem cells from exfoliated deciduous teeth, AI-BMSCs.³⁶ All of these MSCs exhibit self-renewal, multilineage differentiation potential, and immunomodulatory properties.³⁷ Compared to other MSCs, they are highly proliferative, survival properties, and significantly higher osteogenesis *in vitro* and *in vivo*, thus they have great potential advantages of MSC-based regeneration.³⁸ Except these superiors, AI-BMSCs have unique advantages over Lon-BMSCs, such as less invasive and easier harvest procedure (which can be collected during the process of tooth retraction, dental implantation), high proliferation (only 0.1 to 3 mL volume of tissue is needed), high success rate (approximately 70%), more osteogenically responsive.^{15,39} All these characteristics have made AI-BMSCs potentially more desirable for wide therapeutic applications. Although it has been found that AI-BMSCs sheet would increase local bone density when transplanted into the tooth-extraction site,¹⁶ the function of AI-BMSCs sheet *in vitro* and the craniofacial bone

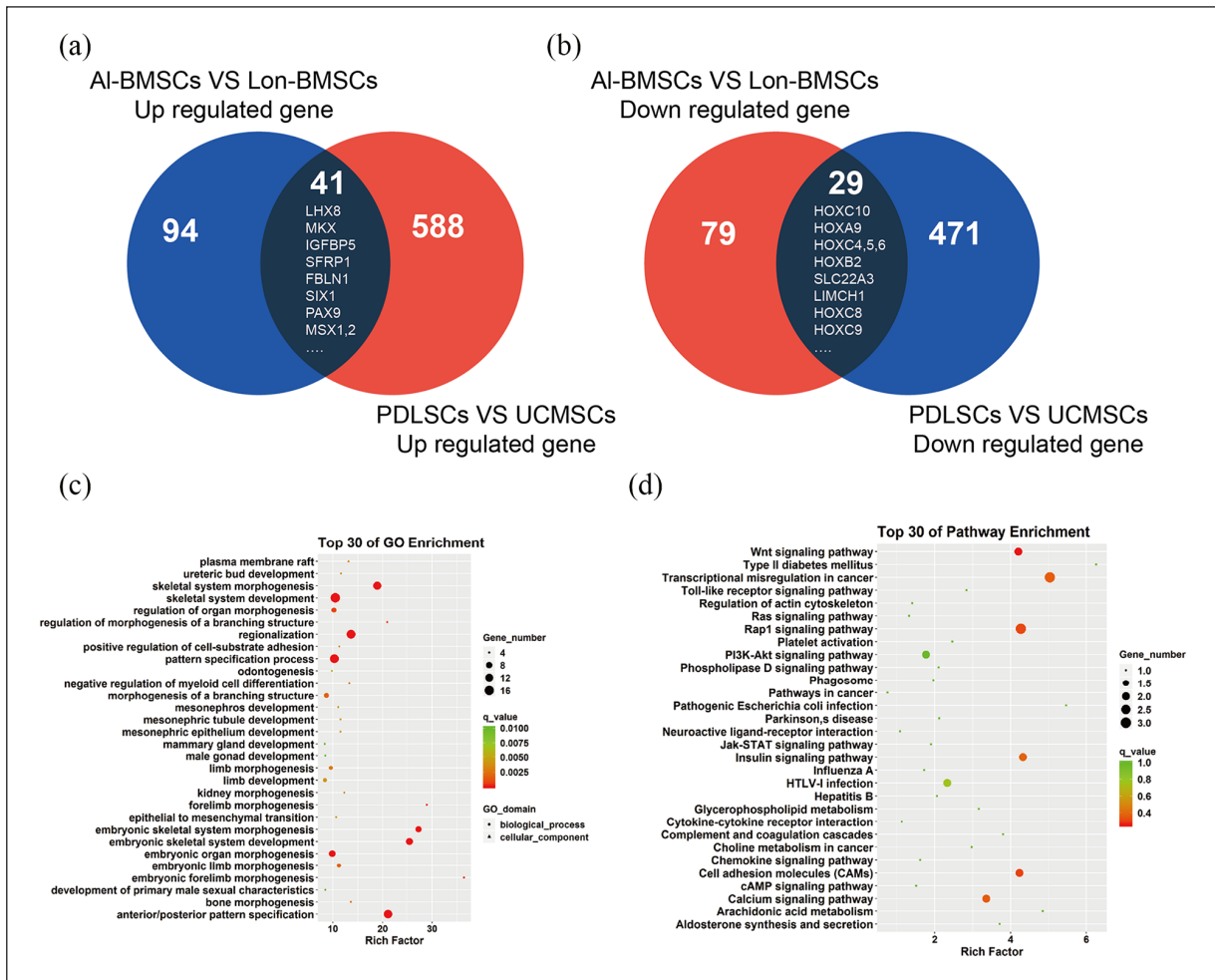


Figure 6. Bioinformatics analysis gene expression profile of Lon-BMSCs and AI-BMSCs. (a, b) Overlap genes from the two profile sets (AI-BMSCs VS Lon-BMSCs, PDLSCs VS UCMSCs), generated using an online tool. Each colored circle represents a different dataset, and areas of overlap indicate shared genes. Statistically significant were defined based on $\text{adj. } P < 0.05$ and $[\text{FC}] > 2$ as the cut-off criteria. (c) GO enrichment analyses of shared genes. The top 30 terms in each GO category. (d) KEGG enrichment analyses of shared genes. The top 30 significant KEGG pathways. GO and KEGG analysis was performed using the DAVID online tool with the cutoff criteria of $\text{FDR} < 0.05$. The color of each bubble represents the FDR for that term, with red representing greater significance. The rich factor refers to the proportion of enriched genes for each term.

defect repairment features *in vivo* remain unclear. Our results showed that AI-BMSCs sheet have the similar histology structure, higher osteogenic differentiation capacity and bone defect reconstruction in rabbit calvarial defect model, demonstrating AI-BMSCs sheet based tissue regeneration would be a promising strategy for craniofacial defect repair in future clinical applications.

Multiple immune cells, such as Th1, Th2, Th17, macrophages, infiltrated into the transplanted area is inevitable, certainly immune cell infiltrated were necessary for tissue regeneration or wound-healing.⁴⁰ At the early stage of 1 week to 1 month during tissue regeneration, it was infiltrated by neutrophils, followed by dense infiltration of monocytes.⁴¹ At the late stage, it was turned to anti-inflammatory cells, like M2 macrophages.⁴² The results of the present study showed the Th1, M1 and M2

have no significantly difference in different groups. This indicating that the immunoregulation function of Lon-BMSCs and AI-BMSCs have no differentiation. Study showed that AI-BMSCs exhibited immunosuppressive effects on monocyte activation and T cell activation and proliferation similar to Lon-BMSCs. Both AI-BMSCs and Lon-BMSCs drove macrophages into an anti-inflammatory M2 phenotype.⁴³

In order to uncover the mechanism of the difference between AI-BMSCs and BMSCs, researchers have performed gene array analyses.⁴⁴ Although lots of differential genes have been found, it was hard to identify the key gene. Thus, we overlapped the differential genes with another gene expression data derived from S Yu et al.,²⁰ which compared the gene expression between another neural crest MSCs, PDLSCs and UCMSCs. The results

showed that the Homeobox genes, like *LHX8*, *MKX*, *PAX9*, *MSX* and *HOX*, were the most significantly differential genes. Homeobox genes contain a small conserved region of DNA consisting of 180 nucleotide base pairs. These genes play an important role in regulating cellular biology by producing proteins that bonded to the DNA of downstream genes.⁴⁵ Homeobox genes are involved in the field of developmental biology, which regulates the multiple germ layers to coordinate the cell division and other cellular functions.⁴⁶ The Homeobox genes were also found to regulate the development of craniofacial tissue, and act as the target gene to manipulate stem cells to become odontogenic fate.⁴⁷ *LHX8* has been known to be associated with facial development in several animals, depletion *LHX8* would lead to orofacial clefts.⁴⁵ The *MSX* genes are critical factors for epithelial-mesenchymal interactions in developmental processes, especially for neural crest specifications and postnatal craniofacial morphogenesis. Deficiency of *Msx1* and *Msx2* would result in severe deformation in mandibular morphogenesis.⁴⁸ *HOX* genes control the proliferation of MSCs and the process of maxillofacial and dental development. Evidence was found that Lon-BMSCs can be differentiated into chondrocytes after transplanted into mandibular defects. The reason was that mandibular microenvironment and AI-BMSCs were *Hox*-negative but they adopted a *Hox*-positive profile when transplanted into a tibia defect. Conversely, Lon-BMSCs were *Hox*-positive and maintain this *Hox* status even when transplanted into a *Hox*-negative mandibular defect.⁴⁹ *Hox* genes are involved in organ formation and regeneration,⁵⁰ a distinct expression of *HOXA5* and *A10*, *HOXB6*, *B7*, *HOXC4*, *C6*, *C8*, *C9* and *C10* as well as *HOXD3* and *D8* is observed in different MSCs.⁵¹

HOX genes have been shown to play critical roles during osteogenesis of human MSCs. Histone demethylase *KDM6B* regulate MSCs osteogenic differentiation by controlling *Hox* expression through histone 3K27 trimethylation (*H3K27me3*).⁵² *HOXB7* can enhance the osteogenic differentiation potential of BMSCs by up-regulating the expression of runt-related transcription factor 2 (*RUNX2*) and directly activating the transcript of bone sialoprotein (*BSP*).⁵³ *HOXA10* contributes to the onset of osteogenesis in MSCs by activating *RUNX2*.⁵⁴ *HOXC10* plays an important role in cell differentiation, proliferation, and morphogenesis, but it can inhibits the osteogenic differentiation potential of MSCs through *Runx2*.⁵⁵ Thus, different homeobox gene may have different regulation function in MSCs, which needs to be further investigated.

Conclusion

In conclusion, the results showed AI-BMSCs sheet have higher osteogenic differentiation and bone defect reconstruction capacity than Lon-BMSCs sheet. Homeobox

genes were upregulated in AI-BMSCs than Lon-BMSCs, demonstrated that Homeobox genes may be the key gene regulated AI-BMSCs biology property. All the results showed that AI-BMSCs sheet based tissue regeneration would be a promising strategy for craniofacial defect repair in future clinical applications.



Declaration of conflicting interests

The author(s) declared no potential conflicts of interest with respect to the research, authorship, and/or publication of this article.

Funding

The author(s) disclosed receipt of the following financial support for the research, authorship, and/or publication of this article: This study was supported by the grant from Beijing Municipal Administration of Hospitals' Youth Program (QML20191504), Beijing Municipal Administration of Hospitals Clinical Medicine Development of Special Funding Support (ZYLX201828).

ORCID iDs

Yanan Liu  <https://orcid.org/0000-0002-3012-2821>
Bin Tian  <https://orcid.org/0000-0001-9560-7371>

Supplemental material

Supplemental material for this article is available online.

References

1. Fretwurst T, Gad LM, Nelson K, et al. Dentoalveolar reconstruction: modern approaches. *Curr Opin Otolaryngol Head Neck Surg* 2015; 23(4): 316–322.
2. Eppley BL, Pietrzak WS and Blanton MW. Allograft and alloplastic bone substitutes: a review of science and technology for the craniomaxillofacial surgeon. *J Craniofac Surg* 2005; 16(6): 981–989.
3. Mao AS and Mooney DJ. Regenerative medicine: current therapies and future directions. *Proc Natl Acad Sci U S A* 2015; 112(47): 14452–14459.
4. Gaihre B, Uswatta S and Jayasuriya AC. Reconstruction of craniomaxillofacial bone defects using tissue-engineering strategies with injectable and non-injectable scaffolds. *J Funct Biomater* 2017; 8(4): 49–67.
5. Wei FL, Qu CY, Song TL, et al. Vitamin C treatment promotes mesenchymal stem cell sheet formation and tissue regeneration by elevating telomerase activity. *J Cell Physiol* 2012; 227(9): 3216–3224.
6. Chen GN, Qi YY, Niu L, et al. Application of the cell sheet technique in tissue engineering. *Biomed Rep* 2015; 3(6): 749–757.
7. Ouyang HW, Cao T, Zou XH, et al. Mesenchymal stem cell sheets revitalize nonviable dense grafts: implications for repair of large-bone and tendon defects. *Transplantation* 2006; 82(2): 170–174.
8. Kawecki F, Clafshenkel WP, Fortin M, et al. Biomimetic tissue-engineered bone substitutes for maxillofacial and craniofacial repair: the potential of cell sheet technologies. *Adv Healthc Mater* 2018; 7(6): e1700919.

9. Chen M, Xu Y, Zhang T, et al. Mesenchymal stem cell sheets: a new cell-based strategy for bone repair and regeneration. *Biotechnol Lett* 2019; 41(3): 305–318.
10. Abdel Meguid E, Ke Y, Ji J, et al. Stem cells applications in bone and tooth repair and regeneration: new insights, tools, and hopes. *J Cell Physiol* 2018; 233(3): 1825–1835.
11. Ma L, Hu J, Cao Y, et al. Maintained properties of aged dental pulp stem cells for superior periodontal tissue regeneration. *Aging Dis* 2019; 10(4): 793–806.
12. Pekovits K, Kröpfl JM, Stelzer I, et al. Human mesenchymal progenitor cells derived from alveolar bone and human bone marrow stromal cells: a comparative study. *Histochem Cell Biol* 2013; 140(6): 611–621.
13. Matsubara T, Suardita K, Ishii M, et al. Alveolar bone marrow as a cell source for regenerative medicine: differences between alveolar and iliac bone marrow stromal cells. *J Bone Miner Res* 2005; 20(3): 399–409.
14. Zhu SJ, Choi BH, Huh JY, et al. A comparative qualitative histological analysis of tissue-engineered bone using bone marrow mesenchymal stem cells, alveolar bone cells, and periosteal cells. *Oral Surg Oral Med Oral Pathol Oral Radiol Endod* 2006; 101(2): 164–169.
15. Mason S, Tarle SA, Osibin W, et al. Standardization and safety of alveolar bone-derived stem cell isolation. *J Dent Res* 2014; 93(1): 55–61.
16. Mu S, Tee BC, Emam H, et al. Culture-expanded mesenchymal stem cell sheets enhance extraction-site alveolar bone growth: an animal study. *J Periodontal Res* 2018; 53(4): 514–524.
17. Ye J, Gong P, Zhou F, et al. Culture and identification of human bone marrow mesenchymal stem cells from alveolar ridge dental implant site. *J Craniofac Surg* 2013; 24(5): 1539–1543.
18. Hu L, Zhao B, Gao Z, et al. Regeneration characteristics of different dental derived stem cell sheets. *J Oral Rehabil*. Epub ahead of print 18 June 2019. DOI: 10.1111/joor.12839.
19. Toosi S, Naderi-Meshkin H, Kalalinia F, et al. Bone defect healing is induced by collagen sponge/polyglycolic acid. *J Mater Sci Mater Med* 2019; 30(3): 33.
20. Yu S, Long J, Yu J, et al. Analysis of differentiation potentials and gene expression profiles of mesenchymal stem cells derived from periodontal ligament and Wharton's jelly of the umbilical cord. *Cells Tissues Organs* 2013; 197(3): 209–223.
21. Rozario T and DeSimone DW. The extracellular matrix in development and morphogenesis: a dynamic view. *Dev Biol* 2010; 341(1): 126–140.
22. Daley WP and Yamada KM. ECM-modulated cellular dynamics as a driving force for tissue morphogenesis. *Curr Opin Genet Dev* 2013; 23(4): 408–414.
23. Pirraco RP, Obokata H, Iwata T, et al. Development of osteogenic cell sheets for bone tissue engineering applications. *Tissue Eng Part A* 2011; 17(11-12): 1507–1515.
24. Yorukoglu AC, Kiter AE, Akkaya S, et al. A concise review on the use of mesenchymal stem cells in cell sheet-based tissue engineering with special emphasis on bone tissue regeneration. *Stem Cells Int* 2017; 2017: 2374161.
25. Lundberg JO. Nitrate transport in salivary glands with implications for NO homeostasis. *Proc Natl Acad Sci U S A* 2012; 109(33): 13144–13145.
26. Akahane M, Shigematsu H, Tadokoro M, et al. Scaffold-free cell sheet injection results in bone formation. *J Tissue Eng Regen Med* 2010; 4(5): 404–411.
27. Nakano K, Murata K, Omokawa S, et al. Promotion of osteogenesis and angiogenesis in vascularized tissue-engineered bone using osteogenic matrix cell sheets. *Plast Reconstr Surg* 2016; 137(5): 1476–1484.
28. Safi IN, Mohammed Ali Hussein B and Al-Shammari AM. In vitro periodontal ligament cell expansion by co-culture method and formation of multi-layered periodontal ligament-derived cell sheets. *Regen Ther* 2019; 11: 225–239.
29. Cao Y, Liu Z, Xie Y, et al. Adenovirus-mediated transfer of hepatocyte growth factor gene to human dental pulp stem cells under good manufacturing practice improves their potential for periodontal regeneration in swine. *Stem Cell Res Ther* 2015; 6: 249.
30. Hu J, Cao Y, Xie Y, et al. Periodontal regeneration in swine after cell injection and cell sheet transplantation of human dental pulp stem cells following good manufacturing practice. *Stem Cell Res Ther* 2016; 7(1): 130.
31. Wei F, Song T, Ding G, et al. Functional tooth restoration by allogeneic mesenchymal stem cell-based bio-root regeneration in swine. *Stem Cells Dev* 2013; 22(12): 1752–1762.
32. Gao ZH, Hu L, Liu GL, et al. Bio-root and implant-based restoration as a tooth replacement alternative. *J Dent Res* 2016; 95(6): 642–649.
33. Nakamura A, Akahane M, Shigematsu H, et al. Cell sheet transplantation of cultured mesenchymal stem cells enhances bone formation in a rat nonunion model. *Bone* 2010; 46(2): 418–424.
34. Lee YC, Chan YH, Hsieh SC, et al. Comparing the osteogenic potentials and bone regeneration capacities of bone marrow and dental pulp mesenchymal stem cells in a rabbit calvarial bone defect model. *Int J Mol Sci* 2019; 20: 5015.
35. Lin J, Shao J, Juan L, et al. Enhancing bone regeneration by combining mesenchymal stem cell sheets with β -TCP/COL-I scaffolds. *J Biomed Mater Res B Appl Biomater* 2018; 106(5): 2037–2045.
36. Zhu Y, Zhang P, Gu RL, et al. Origin and clinical applications of neural crest-derived dental stem cells. *Chin J Dent Res* 2018; 21(2): 89–100.
37. Liu J, Yu F, Sun Y, et al. Concise reviews: characteristics and potential applications of human dental tissue-derived mesenchymal stem cells. *Stem Cells* 2015; 33(3): 627–638.
38. Akintoye SO. The distinctive jaw and alveolar bone regeneration. *Oral Dis* 2018; 24(1-2): 49–51.
39. Wang F, Zhou Y, Zhou J, et al. Comparison of Intraoral Bone Regeneration with Iliac and Alveolar BMSCs. *J Dent Res* 2018; 97(11): 1229–1235.
40. Raphael I, Nalawade S, Eagar TN, et al. T cell subsets and their signature cytokines in autoimmune and inflammatory diseases. *Cytokine* 2014; 74(1): 5–17.
41. Corradetti B, Taraballi F, Minardi S, et al. Chondroitin Sulfate Immobilized on a Biomimetic Scaffold Modulates Inflammation While Driving Chondrogenesis. *Stem Cells Transl Med* 2016; 5(5): 670–682.
42. Wynn TA and Vannella KM. Macrophages in tissue repair, regeneration, and fibrosis. *Immunity* 2016; 44(3): 450–462.
43. Cao C, Tarlé S and Kaigler D. Characterization of the immunomodulatory properties of alveolar bone-derived

- mesenchymal stem cells. *Stem Cell Res Ther* 2020; 11(1): 102.
44. Lee JT, Choi SY, Kim HL, et al. Comparison of gene expression between mandibular and iliac bone-derived cells. *Clin Oral Investig* 2015; 19(6): 1223–1233.
 45. Yıldırım Y, Kerem M, Köroğlu Ç, et al. A homozygous 237-kb deletion at 1p31 identified as the locus for midline cleft of the upper and lower lip in a consanguineous family. *Eur J Hum Genet* 2014; 22(3): 333–337.
 46. Holland PW. Evolution of homeobox genes. *Wiley Interdiscip Rev Dev Biol* 2013; 2(1): 31–45.
 47. Ramanathan A, Srijaya TC, Sukumaran P, et al. Homeobox genes and tooth development: understanding the biological pathways and applications in regenerative dental science. *Arch Oral Biol* 2018; 85: 23–39.
 48. Ishii M, Han J, Yen H, et al. Combined deficiencies of *Msx1* and *Msx2* cause impaired patterning and survival of the cranial neural crest. *Development* 2005; 132(22): 4937–4950.
 49. Leucht P, Kim J, Amasha R, et al. Embryonic origin and Hox status determine progenitor cell fate during adult bone regeneration. *Development* 2008; 135(17): 2845–2854.
 50. Seifert A, Werheid DF, Knapp SM, et al. Role of Hox genes in stem cell differentiation. *World J Stem Cells* 2015; 7(3): 583–595.
 51. Woo CJ, Kharchenko PV, Daheron L, et al. Variable requirements for DNA-binding proteins at polycomb-dependent repressive regions in human HOX clusters. *Mol Cell Biol* 2013; 33(16): 3274–3285.
 52. Ye L, Fan Z, Yu B, et al. Histone demethylases KDM4B and KDM6B promotes osteogenic differentiation of human MSCs. *Cell Stem Cell* 2012; 11(1): 50–61.
 53. Gao RT, Zhan LP, Meng C, et al. Homeobox B7 promotes the osteogenic differentiation potential of mesenchymal stem cells by activating RUNX2 and transcript of BSP. *Int J Clin Exp Med* 2015; 8(7): 10459–10470.
 54. Hassan MQ, Tare R, Lee SH, et al. HOXA10 controls osteoblastogenesis by directly activating bone regulatory and phenotypic genes. *Mol Cell Biol* 2007; 27(9): 3337–3352.
 55. Li G, Han N, Yang H, et al. Homeobox C10 inhibits the osteogenic differentiation potential of mesenchymal stem cells. *Connect Tissue Res* 2018; 59(3): 201–211.